

Article

Genome-Wide and Transcriptome-Wide Association Analysis Identifies *qRS-6D* and Its Candidate Genes Regulating Root Development of Wheat Seedlings

Mingzhu Cheng, Pengcheng Wang, Xueting Liu, Zhiwei Zhu, Sichun Qiu, Yuxiu Liu, Xue Shi, Wanquan Ji, Shengbao Xu and Xiaoming Wang *

State Key Laboratory of Crop Stress Biology for Arid Areas, College of Agronomy, Northwest A&F University, Yangling, Xianyang 712100, China; chengmingzhu@nwfau.edu.cn (M.C.); wangpc@nwfau.edu.cn (P.W.); liuxuet@nwfau.edu.cn (X.L.); zhuzhiwei@nwfau.edu.cn (Z.Z.); qsc@nwfau.edu.cn (S.Q.); liuyuxiu@nwfau.edu.cn (Y.L.); shixue@nwfau.edu.cn (X.S.); jiwantuan2003@126.com (W.J.); xushb@nwfau.edu.cn (S.X.)

* Correspondence: wangxm@nwsuaf.edu.cn

Abstract: Wheat (*Triticum aestivum* L.) is one of the most important cereal crops worldwide, and its production is challenged by global climate change and a shortage of resources. The root system plays a vital role in uptaking water and nutrients and sensing soil environmental signals, and it has great potential to improve the final yield and stress tolerance of wheat. In order to further explore the genes regulating root development, this study focused on *qRS-6D*, located on chromosome 6D and spanning from 462,701,391 to 465,068,943, which was significantly associated with the total root length, root volume, root surface, and root fresh weight in our previous GWAS analysis. Firstly, its genetic effects were validated using an F₆ segregating population by comparing the root-related traits of homologous lines harboring the alternative haplotypes of this QTL. Then, the number of causal genes of this QTL was narrowed down to four with a transcriptome-wide association study. Additionally, *qRS-6D* has been demonstrated to have genetic effects on several yield- (kernel length, kernel width, and thousand-kernel weight) and plant structure-related traits (plant height, peduncle length, total tiller number, productive tiller number, flag leaf length, and flag leaf angle). Relatively, the frequency of the favorable haplotype increased with the wheat breeding practice. This study provides a reliable genetic locus to improve root development and structure and evaluate its application potential in wheat breeding improvement.

Keywords: bread wheat; root system; GWAS; TWAS; population transcriptome



Citation: Cheng, M.; Wang, P.; Liu, X.; Zhu, Z.; Qiu, S.; Liu, Y.; Shi, X.; Ji, W.; Xu, S.; Wang, X. Genome-Wide and Transcriptome-Wide Association Analysis Identifies *qRS-6D* and Its Candidate Genes Regulating Root Development of Wheat Seedlings. *Agronomy* **2024**, *14*, 1075. <https://doi.org/10.3390/agronomy14051075>

Academic Editor: Mirosław Tyrka

Received: 2 April 2024

Revised: 5 May 2024

Accepted: 16 May 2024

Published: 19 May 2024



Copyright: © 2024 by the authors. Licensee MDPI, Basel, Switzerland. This article is an open access article distributed under the terms and conditions of the Creative Commons Attribution (CC BY) license (<https://creativecommons.org/licenses/by/4.0/>).

1. Introduction

Hexaploid bread wheat (*Triticum aestivum* L.), one of the global cereal crops, holds significant importance in ensuring global food security and fostering economic development [1]. However, the increasing global climate change [2], resource shortages, and environmental pollution due to excessive fertilizer and pesticide use [3] pose severe challenges to future wheat production. The root system is vital for absorbing water and soil nutrients and also plays a key role in sensing and responding to environmental stresses [4], such as low temperatures [5], drought [6], and salinity [7]. A well-developed root structure has the potential to enhance plant resilience [8], such as by improving soil nutrient utilization efficiency and reducing water usage [9], thereby increasing the final crop yield under climate change conditions. However, the past genetic improvement efforts in wheat mainly targeted the aboveground traits, including plant height [10], yield components [11], and disease resistance [12], due to the difficulties in observing the root-related traits. Currently, the significance of root improvement has been increasingly recognized, and some have

proposed that improving crop roots could be the key to triggering a second green revolution [13], highlighting the growing importance of genetic dissection of root development and architecture.

In wheat, hundreds of quantitative trait loci (QTLs) controlling root development and architecture have been identified [14]. However, the cloning and breeding applications of these QTLs face significant challenges due to wheat being an allohexaploid with a large genome size (~16 G), comprising three subgenomes (A, B, and D), and exhibiting over 95% similarity in homologous gene sequences among different subgenomes [15]. Additionally, there is a close interaction between root development and environmental conditions. In recent years, the release of the wheat reference genome sequence [16] and the rapid development of methods for cloning genes controlling agricultural traits have facilitated the cloning of genes associated with root development [17]. For instance, the *TaOPR1III* dosage differences can adjust wheat's root structure, with an increased dosage or transgenic over-expression resulting in reduced seminal root growth [18]; *TaVRN1* has been reported to regulate the root angle at all developmental stages of wheat [19]; *TaVSR1-B* shortens the elongation zone of roots, increases the meristematic zone, and promotes longitudinal root growth [20]; *TaMOR* significantly increases root numbers and individual plant yield by regulating secondary root initiation in wheat [21]; *TaEGT1* [22] and *TaEGT2* [23] promote steep root growth by regulating the root growth angle; and *TaSRL1* suppresses wheat root growth by integrating auxin and jasmonic acid signals [24]. Multiple studies have also indicated that genes controlling wheat root development can enhance its resistance to abiotic stress. For example, *TaSINA2B* [25] and *TaOPR1III* [18] enhance drought resistance by regulating the root length and lateral root development; *TaANR1* and *TaMAD25* enhance wheat nitrogen uptake and drought resistance by increasing the primary root length [26]; and *TaSWN* enhances wheat adaptation to low-nitrogen environments by promoting root development [27]. In our previous study, we cloned several root development-related genes with a genome-wide association study (GWAS), including *TaFMO1-5B*, which regulates the total root length and surface area [28]; the "Green Revolution" allele *Rht-D1b* (*reduced height-D1b*), which significantly increases wheat root systems [29]; and *TaGW2-6B* (*grain width2-6B*), whose mutants show enlarged root systems [30].

The genetic network and root structure of wheat root development are highly complex, and currently cloned genes cannot improve root development well. To delve further into the genes governing wheat root development, we directed our attention to a quantitative trait locus (QTL) located on chromosome 6D. This locus exhibited significant associations with the total root length (TRL), root surface (RS), root volume (RV), and fresh root weight (RFW) in our previous genome-wide association study (GWAS) analysis [28]. The genetic effects of this QTL were validated using a bi-parental segregation population. Candidate genes within this locus were prioritized through transcriptome-wide association study (TWAS), and its potential application was evaluated based on collected agricultural traits. These findings establish a dependable genetic locus for regulating wheat root development.

2. Materials and Methods

2.1. Plant Materials

The GWAS population comprised 406 worldwide wheat accessions. Root-related traits were measured 14 days after germination in a hydroponic system with six independent replications [28]. Briefly, in each replication, a minimum of six plants with comparable growth statuses were utilized for phenotyping root-related traits, with one plant designated for root sample collection. The collected root samples were promptly frozen in liquid nitrogen for subsequent RNA isolation. The six independent root samples from the six replications were combined in equal proportions for total RNA extraction and subsequent RNA sequencing.

The bi-parent segregation population used to validate the genetic effects of *qRS-6D* comprised 134 lines of F₆ recombinant inbred lines (RILs) derived from a cross between

Chinese Spring (CS) and MK95. The population was developed with the single-seed descent method and was advanced to the F_6 generation. CS is a landrace used for the whole-genome sequencing of bread wheat [31]. MK95 is a heat-tolerant wheat accession introduced by the International Center for Agricultural Research in the Dry Areas (ICARDA). The root system of MK95 is larger than that of CS. Our population genotype data showed the CS and MK95 harboring $qRS-6D^{HapA}$ and $qRS-6D^{HapB}$, respectively.

2.2. KASP Marker Development for $qRS-6D$

One pair of PCR primers covering SNP-6D-464834393 (the lead SNP for $qRS-6D$ in the GWAS analysis) was designed, and the PCR products were sequenced to validate the sequence polymorphisms between CS and MK95 at this locus. Then, a KASP marker was developed using the online tool PolyMarker (<http://www.polymarker.info/>, accessed on 6 January 2024) [32]. The primer sequences of this marker were as follows: GAA GGT GAC CAA GTT CAT GCT GTT TCC GTT TGG TGC ATT CA for KASP-6D-F; GAA GGT CGG AGT CAA CGG ATT GTT TCC GTT TGG TGC ATT CG for KASP-6D-H; and ACT CAA CTG GAA TCT CGA TAC C for KASP-6D-R.

The reactions were performed in a total volume of 5 μ L, containing 250 ng of template DNA, 2.5 μ L of KASP V4.0 2 \times Master mix (LGC, Teddington, UK), and 0.07 μ L of a mixture of forward and reverse primers. The PCR procedure was as follows: 15 min at 94 $^{\circ}$ C, 45 cycles for 20 s at 94 $^{\circ}$ C, and 60 s at 64–57 $^{\circ}$ C (dropping 0.8 $^{\circ}$ C per cycle). After the reaction was completed, fluorescence scanning was conducted using FLUOstar Omega (BMG Labtech GmbH, Ortenberg, Germany), and genotyping was performed using KlusterCaller software (v3.3.41.0).

2.3. Phenotyping of Root-Related Traits

The 56 homozygous lines of the F_6 RILs identified by the above-developed KASP marker, including 26 $qRS-6D^{HapA}$ lines (155 plants) and 30 $qRS-6D^{HapB}$ lines (183 plants), were utilized for phenotyping root-related traits. Sixteen seeds of similar sizes were selected for each line, sterilized with 2% sodium hypochlorite for 10 min, and then rinsed 3–5 times with distilled water. The sterilized seeds of each line were incubated at 4 $^{\circ}$ C in darkness for two days to break dormancy. Then, they were placed on damp filter papers in a germination box (12 \times 12 \times 5 cm), which were cultivated under 22 $^{\circ}$ C/16 $^{\circ}$ C day/night (50% relative air humidity) and 16 h light (2000 Lux)/8 h dark cycles for 14 days.

At least six plants with consistent development statuses for each line were selected for phenotyping the TRL (cm), RS (cm²), and RV (cm³) with the Wseen LA-S image system (Hangzhou Wseen Testing Technology Co. LTD., Hangzhou, China). The PRL (cm) was measured with a ruler, and the FRW (g) was weighed.

2.4. Haplotype Analysis of $qRS-6D$

LD block analysis was performed using Plink software (v1.90b6.20). Based on the LD block analysis results, the haplotype was determined with the significant SNPs in the GWAS analysis. The R (v4.0.1) heatmap package was utilized for visualization.

2.5. Screening of Candidate Genes for $qRS-6D$

The gene expression levels in the $qRS-6D$ interval were investigated with the population transcriptomes, and genes with average transcripts per million (TPM) values >0.5 across the 406 accessions were filtered as expressed genes in wheat root. The quantified expression of each gene in each accession could be searched for in and downloaded from our database (<https://resource.iwheat.net/WGPD/>, accessed on 16 February 2024). Then, the association between the expression variations of the expressed genes and the phenotype of root-related traits was found with a TWAS. The TWAS was conducted with our newly developed method (unpublished data), in which the mixed linear model, the fundamental model in the GWAS, was employed to exploit the continuous gene expression variations

and exclude the inference of the population structure and family relatedness with the lmerTest (v3.1.3) package in R (v 4.2.2).

2.6. Identification of Differentially Expressed Genes

The 406 accessions were categorized into two groups based on the two haplotypes of *qRS-6D*, including 219 *qRS-6D*^{HapA} accessions and 187 *qRS-6D*^{HapB} accessions. Then, the expression levels of each gene expressed in the wheat roots were compared between the two groups using a mixed linear model that accounted for the population structure and familial relatedness, as described in our previous method [28]. Only genes with TPM values >0.5 in at least 20 accessions were applied to the analysis. The genes with a fold change ≥ 1.2 (p value < 0.01) and average expression values >0.5 in both of the compared groups were considered differentially expressed genes.

2.7. GO Enrichment Analysis

The Triticeae-GeneTribe website (<http://wheat.cau.edu.cn/TGT/>, accessed on 10 March 2024) and Chinese Spring's reference genome (IWGSC RefSeq v2.1) were used for conducting GO enrichment analysis [33]. The p values were adjusted for multiple tests by Benjamini and Hochberg. The R (v4.0.1) ggplot2 package was used to visualize the enrichment results.

3. Results

3.1. Identification and Haplotype Assignment of *qRS-6D*

In our prior study, GWAS analysis identified 46 loci significantly associated with root-related traits [28]. Here, we specifically examined the locus situated on chromosome 6D, which exhibited significant associations with the TRL, RS, RV, and RFW, explaining 6.78%, 15.22%, 24.13%, and 23.17% of the phenotype variations, respectively (Figure 1a). Considering the effects of the grain size and weight on the root-related traits of wheat seedlings, we excluded these effects with the general linear model and reperformed the GWAS analysis with the corrected phenotype values. The results showed that this locus remained significantly associated with the corrected TRL, RS, RV, and RFW phenotypes, explaining 6.37%, 11.93%, 20.96%, and 18.71% of the phenotype variations, respectively (Figure S1). Linkage disequilibrium (LD) analysis between the significantly associated SNPs and their flanking SNPs indicated that the physical interval ranged from 462,701,391 to 465,068,943 (Figure 1b). This locus is named *qRS-6D* hereafter.

Haplotype analysis divided the significantly associated SNPs into two major haplotypes, namely *qRS-6D*^{HapA} (AAGCAAGTAGC) and *qRS-6D*^{HapB} (CGCTCGTGGAG), with frequencies of 53.94% and 46.06%, including 219 *qRS-6D*^{HapA} accessions and 187 *qRS-6D*^{HapB} accessions, respectively (Table 1). The phenotype values of the TRL, RS, RV and FRW exhibited significant differences between accessions harboring *qRS-6D*^{HapA} and *qRS-6D*^{HapB}, which increased by 6.62%, 9.62%, 13.06% and 10.85%, respectively, in the *qRS-6D*^{HapB} genotypes compared with the *qRS-6D*^{HapA} genotypes (Figure 1c).

Table 1. The haplotypes determined by the significantly associated and closely linked SNPs in the *qRS-6D* interval.

Haplotype	Sequence	Total Root Length (TRL, cm)	Root Surface (RS, cm ²)	Root Volume (RV, cm ³)	Fresh Root Weight (RFW, g)	Frequency
HapA	AAGCAAGTAGC	65.24 ± 11.20	6.63 ± 1.11	0.056 ± 0.01	0.08 ± 0.02	53.94%
HapB	CGCTCGTGGAG	69.56 ± 9.97	7.27 ± 1.15	0.063 ± 0.01	0.09 ± 0.01	46.06%

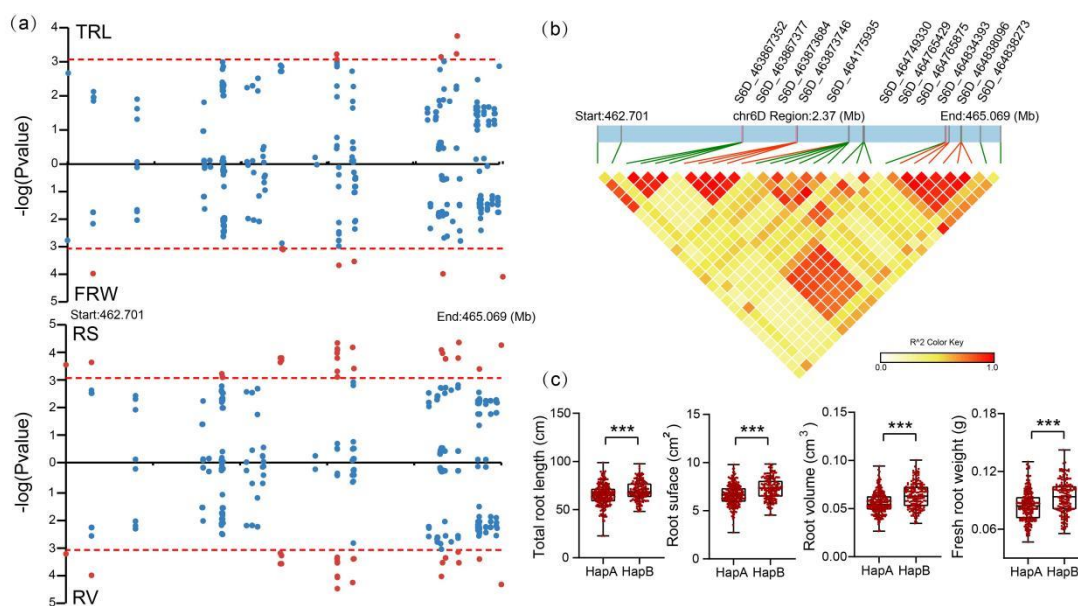


Figure 1. Identification and haplotype analysis of *qRS-6D*. (a) Manhattan plots of the SNPs located in the *qRS-6D* interval in the GWAS analysis. The red horizontal line indicates the threshold of significance used in the GWAS ($p = 8.58 \times 10^{-4}$). The red and blue circles indicate significant and insignificant SNPs in the GWAS, respectively. “TRL”, “FRW”, “RS”, and “RV” represent the total root length, root surface, root volume, and fresh root weight, respectively. (b) Linkage disequilibrium (LD) heatmap of SNPs located in the *qRS-6D* interval. The red lines indicate the SNPs closely linked and used for the haplotype assignment. (c) The accessions harboring alternative haplotypes showed significantly different root-related traits. *** Student’s *t*-test $p < 0.001$.

3.2. Experimental Validation of the Genetic Effects of *qRS-6D*

To validate the genetic effects of *qRS-6D* on root development, we constructed a biparental F_6 recombinant inbred population (RIL) by crossing Chinese Spring (CS) and MK95, which belong to the *qRS-6D*^{HapA} and *qRS-6D*^{HapB} haplotypes, respectively, and exhibited significantly different TRL, RS and RV values (Figure 2a,b). The sequence polymorphisms surrounding the lead SNP (SNP-6D-464834393) identified in the GWAS analysis between the two parent lines were validated with PCR product sequencing (Figure S2). A Kompetitive Allele-Specific PCR (KASP) marker was developed to discriminate the genotype at the lead SNP (SNP-6D-464834393) position and successfully divide the RIL lines into two groups (Figure 2c). Then, the homozygous lines were used for phenotyping the root-related traits, and the results showed that the phenotypes were significantly different between the lines harboring the *qRS-6D*^{HapA} and *qRS-6D*^{HapB} haplotypes. The TRL, RS, and RV values of the *qRS-6D*^{HapB} lines increased by 8.16%, 7.52%, and 7.20%, respectively, compared with the *qRS-6D*^{HapA} lines (Figure 2d). These results experimentally validate the genetic effects of *qRS-6D* on the TRL, RS, and RV.

3.3. Screening of the Candidate Genes of *qRS-6D*

Based on the annotation of Chinese Spring’s reference genome (IWGSC RefSeq v2.1), 70 high-confidence genes were found within the *qRS-6D* interval. Through investigation of the population transcriptome, 24 genes expressed in wheat roots with an average TPM > 0.5 across the 406 accessions (Table S1). Then, a TWAS was performed to screen the candidate genes of *qRS-6D* by associating the expression levels of the above 24 genes with the phenotype variations in the TRL, RS, RV and RFW (Table S2). Four genes, *TraesCS6D02G385100*, *TraesCS6D02G385600*, *TraesCS6D02G388400*, and *TraesCS6D02G388700*, were identified to be significantly associated with all of the four investigated traits (Figure 3a, Table S2, and Figure S3). The highest and lowest significance levels were from associations between

TraesCS6D02G388400 and the RV (p value = 1.3×10^{-4}) and between *TraesCS6D02G385100* and the RFW (p value = 4.18×10^{-2}), respectively.

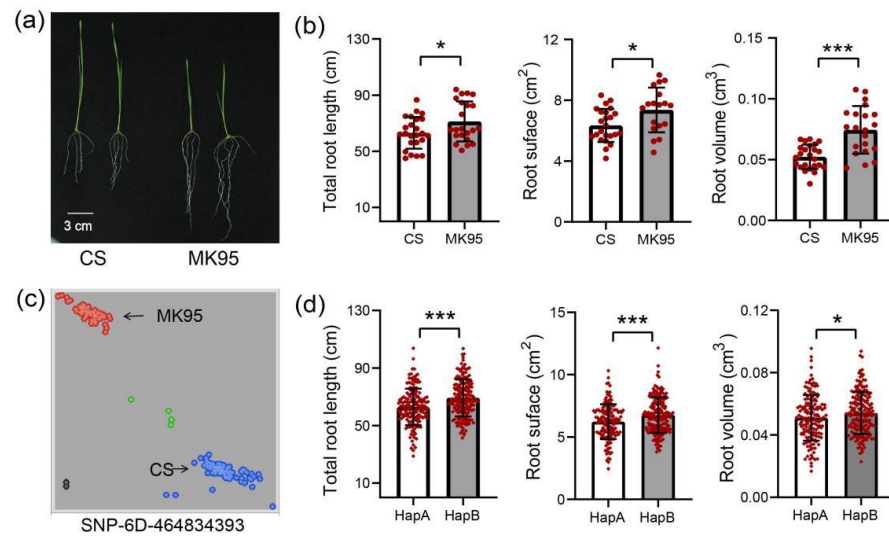


Figure 2. The genetic effect validation of *qRS-6D* with F_6 segregation populations. (a,b) The phenotype (a) and statistical comparisons (b) of root-related traits between the two parent lines of the F_6 segregation populations. (c) The genotyping of the lines from the F_6 segregation populations with the developed KASP marker. Blue and red dots indicate the two homozygous genotypes at the lead SNP position. Green dots indicate the heterozygous genotypes. Black dots represent the non-template control (NTC). (d) The statistical comparisons of the root-related traits between lines harboring the *qRS-6D*^{HapA} and *qRS-6D*^{HapB} haplotypes. * and *** indicate the significance level of Student’s *t*-test at $p < 0.05$ and $p < 0.001$, respectively.

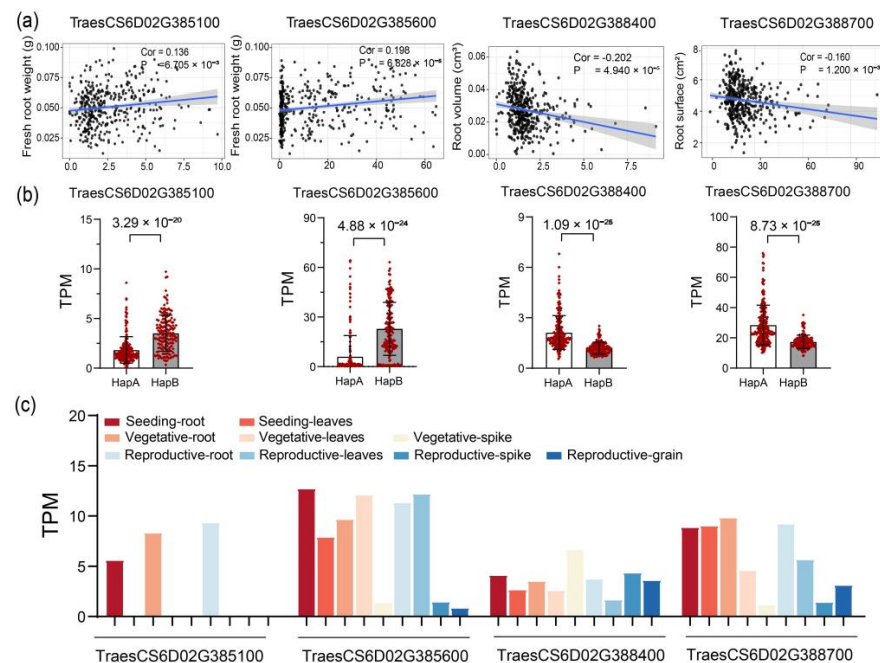


Figure 3. The association analysis and the expression levels of the four candidate genes. (a) The correlation between gene expression levels and phenotype variations. The correlation coefficients and p values were calculated using Pearson correlation analysis. (b) The difference in expression levels of the four candidate genes between *qRS-6D*^{HapA} and *qRS-6D*^{HapB} genotypes calculated with the Student’s *t*-test. (c) The expression levels of the four candidate genes among wheat organs (<http://wheatomics.sdau.edu.cn/expression/wheat.html>, accessed on 3 March 2024).

For *TraesCS6D02G385100*, its expression levels were significantly different between the accessions harboring the *qRS-6D^{HapA}* and *qRS-6D^{HapB}* haplotypes (Figure 3b). The significance levels in the TWAS analysis were 2.97×10^{-2} , 2.13×10^{-2} , 2.30×10^{-2} , and 4.18×10^{-2} for the TRL, RS, RV and RFW, respectively. Its average expression level was 2.53 in terms of TPM, ranging from 0 to 9.72, and the expression breadth was 95.32%, meaning this gene was expressed in 95.32% of the 406 accessions (TPM > 0.5). Publicly available RNA-seq data reveal that this gene is expressed in the roots during both the vegetative and reproductive development stages, with lower expression levels observed in the leaves and grains (Figure 3c). *TraesCS6D02G385100* encodes LRR receptor-like serine/threonine-protein kinase EFR. This may involve reducing rhizobia radiata transformation by inducing plant defenses to modulate the immune response [34].

For *TraesCS6D02G385600*, its expression levels were significantly different between the accessions harboring the *qRS-6D^{HapA}* and *qRS-6D^{HapB}* haplotypes (Figure 3b). The significance levels in the TWAS analysis were 3.27×10^{-2} , 4.81×10^{-2} , 3.48×10^{-3} , and 1.52×10^{-3} for the TRL, RS, RV, and RFW, respectively. Its average expression level was 13.77 in terms of TPM, ranging from 0.04 to 64.63, and the expression breadth was 96.55%. Publicly available RNA-seq data show that this gene is expressed in the roots, leaves, and grains during the vegetative and reproductive development stages, with a higher level in seedling roots (Figure 3c). *TraesCS6D02G385600* encodes Silicon efflux transporter LSI2. It mainly participates in the transport of silicon from root cells to the apoplast, coupled with the NIP2-1/LSI1 transport protein at the root, to efficiently absorb arsenite, thereby promoting plant growth and enhancing resistance to pests, diseases, and other stresses [35,36].

For *TraesCS6D02G388400*, its expression levels were significantly different between the accessions harboring the *qRS-6D^{HapA}* and *qRS-6D^{HapB}* haplotypes (Figure 3b). The significance levels in the TWAS analysis were 1.33×10^{-2} , 2.01×10^{-4} , 1.30×10^{-4} , and 1.99×10^{-2} for the TRL, RS, RV and RFW, respectively. Its average expression level was 1.723 in terms of TPM, ranging from 0 to 9.124, and the expression breadth was 97.78%. Publicly available RNA-seq data indicate that this gene is expressed in the roots, leaves, and grains during both the vegetative and reproductive development stages, with a higher level observed in seedling roots (Figure 3c). *TraesCS6D02G388400* encodes a DDL protein with a conserved Forkhead-associated (FHA) domain [37]. The mutants of its homolog in *Arabidopsis* showed delayed development and defects in the root, stem, and flower organs, shortened root meristematic zones, shorter roots, and reduced cell division and cell numbers [37].

For *TraesCS6D02G388700*, its expression levels were significantly different between the accessions harboring the *qRS-6D^{HapA}* and *qRS-6D^{HapB}* haplotypes (Figure 3b). The significance levels in the TWAS analysis were 8.14×10^{-4} , 4.90×10^{-4} , 6.48×10^{-3} , and 3.58×10^{-2} for the TRL, RS, RV and RFW, respectively. Its average expression level was 23.87 in terms of TPM, ranging from 2.04 to 106.49, and the expression breadth was 100%. Publicly available RNA-seq data show that this gene is expressed in the roots, leaves, and grains during the vegetative and reproductive development stages. However, its expression level was higher in the roots (Figure 3c). *TraesCS6D02G388700* encodes caffeic acid 3-O-methyltransferase (COMT). The lead SNP of *qRS-6D*, SNP-6D-464765429, causes a missense mutation and is located on the first exon of this gene. COMT is a crucial enzyme in lignin biosynthesis which promotes plant growth, tissue development, organ development, lodging resistance, and responses to various stresses [38]. Recent findings showed that mutations in *bmr12* encoding sorghum caffeic acid O-methyltransferase reduced the lateral root density and altered the root anatomy [39].

3.4. The Mechanisms Underlying *qRS-6D* Revealed by a Population Transcriptome

To understand the mechanisms underlying the genetic effects of *qRS-6D* on root development, we identified the differential expression genes (DEGs) between the *qRS-6D^{HapA}* and *qRS-6D^{HapB}* genotypes with a mixed linear model, in which the population structure

and potential familial relatedness were accounted for by referring our previously developed method [28]. A total of 12,108 DEGs were identified with the criteria of a p value < 0.01 and fold change ≥ 1.2 , including 4189 upregulated and 7919 downregulated genes in the $qRS-6D^{HapA}$ genotypes compared with the $qRS-6D^{HapB}$ genotypes (Figure 4a and Table S3).

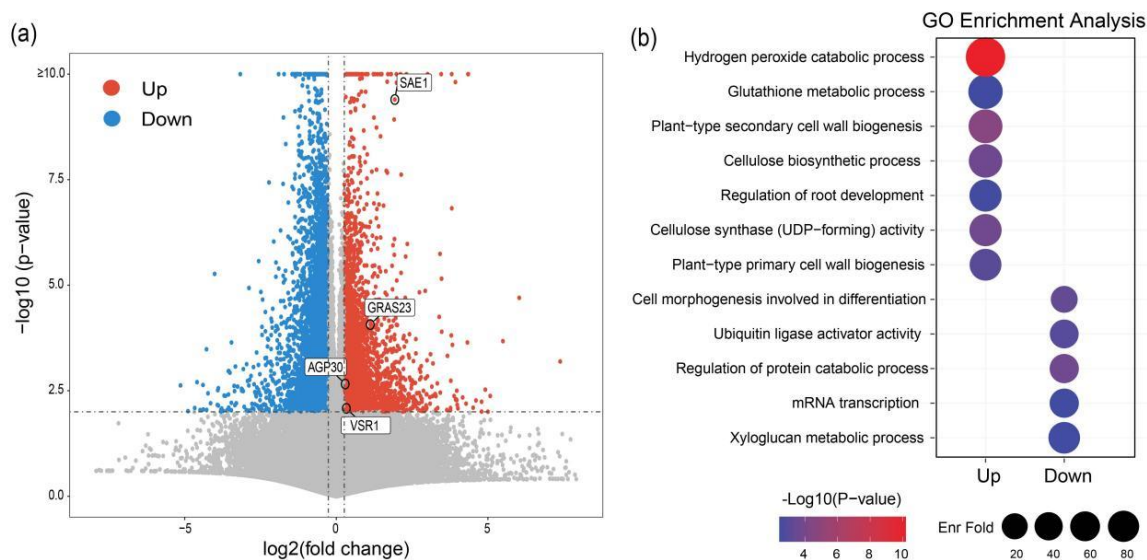


Figure 4. Population transcriptomes revealed molecular mechanisms underlying $qRS-6D$'s effect. (a) Identification of differential expression genes between $qRS-6D^{HapA}$ and $qRS-6D^{HapB}$ genotypes with the mixed linear model. (b) Gene ontology enrichment for the significantly up- and downregulated genes. “EnrFold” represents the enrichment fold. The detailed information is included in Tables S3 and S4.

Among the DEGs, several wheat homologs have been reported to be involved in root development in Arabidopsis and rice, such as *AtAGP30* [40], *AtVSR1* [20], *OsSAE1* [41], and *OsGRAS23* [42]. Gene ontology (GO) enrichment analysis revealed that the biological pathways “hydrogen peroxide catabolic process”, “glutathione metabolic process”, “plant-type secondary cell wall biogenesis”, “regulation of root development”, and “plant-type primary cell wall biogenesis” were significantly enriched for the upregulated genes. In contrast, the GO terms of “cell morphogenesis involved in differentiation”, “ubiquitin ligase activator activity”, “regulation of protein catabolic process”, and “xyloglucan metabolic process” were significantly enriched for downregulated genes (Figure 4b and Table S3). These terms were closely related to root development in model plants [43], providing valuable information for further investigation of the genetic effect of $qRS-6D$ on root development.

3.5. The Pleiotropism of $qRS-6D$

To assess the potential application value of $qRS-6D$ in wheat breeding, its effects on agronomic traits were investigated using phenotype data collected from seven environments [44]. Significant differences were detected between the accessions harboring $qRS-6D^{HapA}$ and $qRS-6D^{HapB}$ for several agronomic traits, including yield- and plant architecture-related traits, which are typical targets for breeding improvement. The accessions harboring $qRS-6D^{HapB}$ exhibited kernel lengths, kernel widths, and thousand-kernel weights which significantly increased by 1.84%, 3.56%, and 5.94%, respectively, compared with the accessions harboring $qRS-6D^{HapA}$. For the plant architecture-related traits, the $qRS-6D^{HapB}$ accessions significantly decreased the plant height, peduncle length, total tiller number, productive tiller number, flag leaf length, and flag leaf angle by 11.69%, 9.98%, 12.79%, 11.86%, 6.52%, and 4.66%, respectively, compared with the $qRS-6D^{HapA}$ accessions (Figure 5), suggesting that $qRS-6D$ also has genetic effects on these above-ground traits.

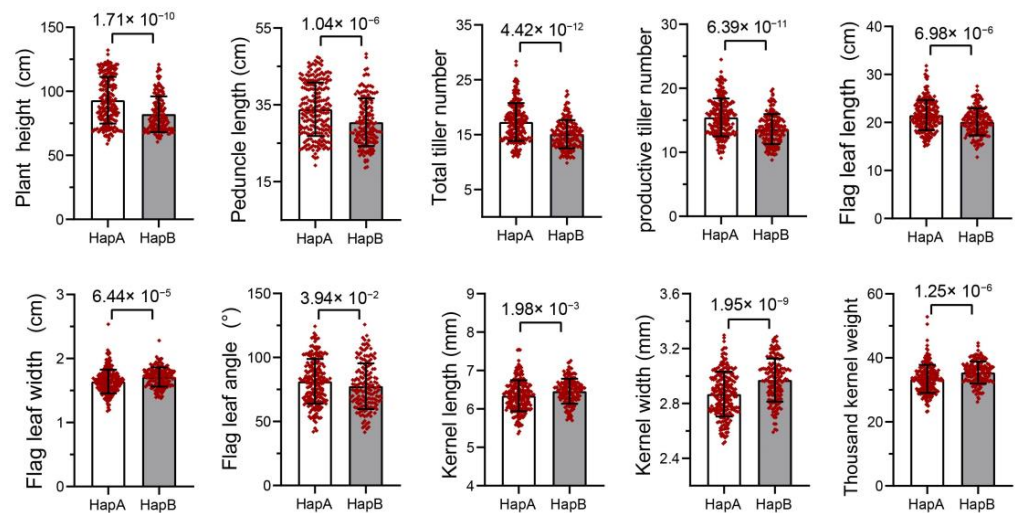


Figure 5. The effects of $qRS-6D$ on different agronomic traits. Statistical significance was determined by the mixed linear model, in which the population structure was added as a fixed effect.

3.6. $qRS-6D^{HapB}$ Frequency Increased with the Wheat Breeding Process

Considering the positive effects of $qRS-6D^{HapB}$ on yield- and plant architecture-related traits, we wondered whether this haplotype was targeted during wheat breeding. We investigated the frequencies of $qRS-6D^{HapB}$ in Chinese cultivars released in different years. The results showed that the frequency of $qRS-6D^{HapB}$ in the modern cultivars (52.78%) was generally higher than that in landrace (16.28%), and it has largely increased since the 1990s (Figure 6a). Aside from that, the frequencies of $qRS-6D^{HapB}$ varied among different ecological regions of wheat production in China. Specifically, in the Yellow River and Huai River valleys' facultative wheat zones, middle and lower Yangtze valley, and the southwestern autumn-sown spring wheat zone (Figure 6b), the frequencies of $qRS-6D^{HapB}$ were higher than those of $qRS-6D^{HapA}$, while in the northern winter wheat zone, the frequency of $qRS-6D^{HapB}$ was lower compared with $qRS-6D^{HapA}$, suggesting that the utilization of $qRS-6D^{HapB}$ may be associated with local ecological conditions.

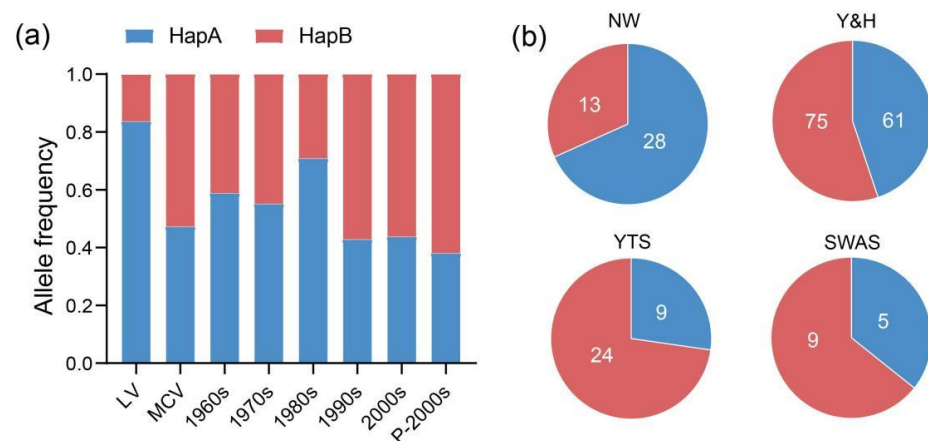


Figure 6. $qRS-6D^{HapB}$ frequency changes with the wheat breeding process. (a) Frequencies of $qRS-6D^{HapA}$ and $qRS-6D^{HapB}$ haplotypes in modern cultivars released from the 1960s to the 2000s. "LV" and "MCV" represent landraces and modern cultivars, respectively. P-2000s represents the period after the 2000s. (b) Frequencies of $qRS-6D^{HapA}$ and $qRS-6D^{HapB}$ haplotypes among Chinese ecological wheat zones. "NW", "Y&H", "YTS", and "SWAS" represent the northern winter wheat zone, the Yellow River and Huai River valleys' facultative wheat zones, the middle and lower Yangtze valley, and the southwestern autumn-sown spring wheat zone, respectively.

4. Discussion

In this study, we validated *qRS-6D*'s genetic effects, narrowed the number of its candidate genes to four with a TWAS, investigated the molecular mechanisms underlying *qRS-6D*'s genetic effects, and evaluated its application potential with collected agricultural traits. Bread wheat is a hexaploid, consisting of three subgenomes, and containing more than 80% repeat sequences in its genome. The sequence similarity among the three subgenomes is more than 95% [15]. That aside, the linkage disequilibrium in wheat is larger than those in other crops. These factors challenged the QTL mapping and the determination of causal genes in the target QTL intervals. At present, the amount of genomic and multi-omics data in wheat has increased rapidly, providing invaluable resources to accelerate functional genomic studies in wheat. In this study, we integrated the genomic and transcriptomic data, GWAS, linkage analysis, and below-ground and above-ground traits to comprehensively understand *qRS-6D*, providing a reference for how to exploit the existing resources efficiently.

The physical interval of *qRS-6D* was determined to be located between 462,701,391 and 465,068,943 in our analysis, which partially overlapped with two previously reported QTLs: one represented by the molecular marker AX-110837768 (464.84 Mb) [45] and another one located between 463.54 Mb and 472.27 Mb [46]. These two QTLs were observed to be significantly associated only with the average root diameter, explaining 8.37% and 9.15% of the phenotypic variation, respectively. In contrast, *qRS-6D* was significantly associated with the TRL, RS, RV, and RFW in our analysis. The overlapping highlights the reliability of our GWAS analysis. More importantly, the candidate genes were narrowed down to *TraesCS6D02G385100*, *TraesCS6D02G385600*, *TraesCS6D02G388400*, and *TraesCS6D02G388700*. With gene transformation or CRISPR-Cas9 gene editing, this QTL will be cloned soon.

The root-related traits of wheat mainly include the TRL, RS, RV, and RFW, root diameter, and number of root tips. Among these, the root dry weight, root volume, and root surface are three representative parameters used to assess a root system's size [47]. The significant association of *qRS-6D* with the TRL, RS, RV, and RFW may be attributed to pleiotropic effects of the same gene or a shared genetic basis among these root-related traits, which aligns with the findings of Savannah Beyer [48]. It is worth noting that *qRS-6D* also has genetic effects on several yield components and plant architecture-related traits, which are the typical traits targeted by wheat breeding. Together with the evidence that the frequency of favorable *qRS-6D*^{HapB} increased with the breeding process, we supposed that the selection of this haplotype contributed to the final yield improvement by optimizing the root development and architecture, consistent with our recent finding that wheat breeding selection synergistically improves above- and below-ground traits [30].

Interestingly, the increased frequency of the *qRS-6D*^{HapB} haplotype in modern cultivars was observed exclusively in the Yellow River and Huai River valleys' facultative wheat zones, middle and lower Yangtze valley, and the southwestern autumn-sown spring wheat zone among Chinese wheat production zones. This indicates a wider adaptability of this favorable haplotype and underscores its potential application value for future wheat breeding endeavors in China.

5. Conclusions

This study validated the genetic effects of the previously identified locus *qRS-6D* with an F₆ segregating population, which is significantly associated with TRL, RS, RV, and RFW, and identified its four candidate genes with TWAS analysis. Additionally, the favorable haplotype *qRS-6D*^{HapB} also improved the yield component and plant architecture-related traits, and the frequency of this haplotype increased with the wheat breeding process, suggesting its application value for future wheat breeding. In conclusion, this study provided a reliable genetic locus for improving the root development and architecture of wheat.

Supplementary Materials: The following supporting information can be downloaded at <https://www.mdpi.com/article/10.3390/agronomy14051075/s1>. Figure S1: The Manhattan plots of SNPs located within the *qRS-6D* interval in the GWAS analysis with the normalized phenotypes for TRL (U_TRL), RS (U_RS), RV (U_RV), and RFW (U_RFW). The red horizontal line indicates the threshold of significance level used in the GWAS ($p = 8.58 \times 10^{-4}$). The red and blue circles indicate significant and insignificant SNPs in the GWAS, respectively. Figure S2: Sequence polymorphism between the two parental lines at SNP-6D-464834393. (a) The flanking sequence of SNP-6D-464834393 was PCR-amplified and sequenced to verify the polymorphism between parent lines at this SNP position. The arrows indicate the SNP positions. (b) Primer information used to amplify the flanking sequence of the target SNP loci. Figure S3: The correlation between candidate gene expression levels and phenotype variations calculated with Pearson correlation analysis. Table S1: Expression levels of the genes located in the *qRS-6D* interval. The expression levels (TPM) were calculated from our previous root population RNA-seq data sampled 14 days after germination. Table S2: TWAS results of genes within the *qRS-6D* interval. Table S3: The identified DEGs between *qRS-6D*^{HapA} and *qRS-6D*^{HapB} genotypes. “UP” and “DOWN” indicate the upregulated and downregulated genes in the *qRS-6D*^{HapA} genotypes, respectively. “HapA_TPM” and “HapB_TPM” indicate the average TPM in the *qRS-6D*^{HapA} and *qRS-6D*^{HapB} genotypes, respectively. Table S4: Gene ontology enrichment of the identified DEGs. GO terms were filtered with p values < 0.05. “UP” and “DOWN” indicate the upregulated and downregulated genes in the *qRS-6D*^{HapA} genotypes compared with the *qRS-6D*^{HapB} genotypes, respectively.

Author Contributions: X.W. and S.X. designed the research; M.C. validated the genetic effects of *qRS-6D*; P.W., Y.L. and S.Q. evaluated the effects of *qRS-6D* on agriculture traits; M.C., X.L. and Z.Z. conducted the DEG analysis, haplotype frequency investigation, and TWAS analysis; X.W. wrote and revised the manuscript; S.X., X.S. and W.J. provided critical suggestions for the data analysis and manuscript writing. All authors have read and agreed to the published version of the manuscript.

Funding: This work was supported by grants from the China Postdoctoral Science Foundation (2021T140566).

Data Availability Statement: The phenotype and genotype data are free to download at <https://iwheat.net/resource/> (accessed on 28 March 2024).

Acknowledgments: The authors thank High-Performance Computing of NWFU for their support.

Conflicts of Interest: The authors declare no conflicts of interest.

References

- Liu, J.; Zhang, Q.; Meng, D.; Ren, X.; Li, H.; Su, Z.; Zhang, N.; Zhi, L.; Ji, J.; Li, J.; et al. *QMrl-7B* Enhances Root System, Biomass, Nitrogen Accumulation and Yield in Bread Wheat. *Plants* **2021**, *10*, 764. [[CrossRef](#)]
- Pugh, T.A.; Müller, C.; Elliott, J.; Deryng, D.; Folberth, C.; Olin, S.; Schmid, E.; Arneth, A. Climate analogues suggest limited potential for intensification of production on current croplands under climate change. *Nat. Commun.* **2016**, *7*, 12608. [[CrossRef](#)] [[PubMed](#)]
- Alori, E.T.; Glick, B.R.; Babalola, O.O. Microbial Phosphorus Solubilization and Its Potential for Use in Sustainable Agriculture. *Front. Microbiol.* **2017**, *8*, 971. [[CrossRef](#)] [[PubMed](#)]
- Lin, Z.; Wang, Y.L.; Cheng, L.S.; Zhou, L.L.; Xu, Q.T.; Liu, D.C.; Deng, X.Y.; Mei, F.Z.; Zhou, Z.Q. Mutual regulation of ROS accumulation and cell autophagy in wheat roots under hypoxia stress. *Plant Physiol. Biochem.* **2021**, *158*, 91–102. [[CrossRef](#)] [[PubMed](#)]
- Peng, L.N.; Xu, Y.Q.; Wang, X.; Feng, X.; Zhao, Q.Q.; Feng, S.S.; Zhao, Z.Y.; Hu, B.Z.; Li, F.L. Overexpression of paralogues of the wheat expansin gene *TaEXPA8* improves low-temperature tolerance in Arabidopsis. *Plant Biol.* **2019**, *21*, 1119–1131. [[CrossRef](#)] [[PubMed](#)]
- Zhou, Y.; Liu, J.; Guo, J.; Wang, Y.; Ji, H.; Chu, X.; Xiao, K.; Qi, X.; Hu, L.; Li, H.; et al. *GmTDN1* improves wheat yields by inducing dual tolerance to both drought and low-N stress. *Plant Biotechnol. J.* **2022**, *20*, 1606–1621. [[CrossRef](#)] [[PubMed](#)]
- Quan, X.; Liang, X.; Li, H.; Xie, C.; He, W.; Qin, Y. Identification and Characterization of Wheat Germplasm for Salt Tolerance. *Plants* **2021**, *10*, 268. [[CrossRef](#)] [[PubMed](#)]
- de Vries, F.T.; Griffiths, R.I.; Knight, C.G.; Nicolitch, O.; Williams, A. Harnessing rhizosphere microbiomes for drought-resilient crop production. *Science* **2020**, *368*, 270–274. [[CrossRef](#)] [[PubMed](#)]
- Ibrahim, S.; Ahmad, N.; Kuang, L.; Li, K.; Tian, Z.; Sadau, S.B.; Tajo, S.M.; Wang, X.; Wang, H.; Dun, X. Transcriptome analysis reveals key regulatory genes for root growth related to potassium utilization efficiency in rapeseed (*Brassica napus* L.). *Front. Plant Sci.* **2023**, *14*, 1194914. [[CrossRef](#)]

10. Tian, X.; Xia, X.; Xu, D.; Liu, Y.; Xie, L.; Hassan, M.A.; Song, J.; Li, F.; Wang, D.; Zhang, Y.; et al. Rht24b, an ancient variation of *TaGA2ox-A9*, reduces plant height without yield penalty in wheat. *New Phytol.* **2022**, *233*, 738–750. [[CrossRef](#)]
11. Ma, S.; Wang, M.; Wu, J.; Guo, W.; Chen, Y.; Li, G.; Wang, Y.; Shi, W.; Xia, G.; Fu, D.; et al. WheatOmics: A platform combining multiple omics data to accelerate functional genomics studies in wheat. *Mol. Plant* **2021**, *14*, 1965–1968. [[CrossRef](#)] [[PubMed](#)]
12. Devanna, B.N.; Jaswal, R.; Singh, P.K.; Kapoor, R.; Jain, P.; Kumar, G.; Sharma, Y.; Samantaray, S.; Sharma, T.R. Role of transporters in plant disease resistance. *Physiol. Plant* **2021**, *171*, 849–867. [[CrossRef](#)] [[PubMed](#)]
13. Den Herder, G.; Van Isterdael, G.; Beeckman, T.; De Smet, I. The roots of a new green revolution. *Trends Plant Sci.* **2010**, *15*, 600–607. [[CrossRef](#)] [[PubMed](#)]
14. Soriano, J.M.; Alvaro, F. Discovering consensus genomic regions in wheat for root-related traits by QTL meta-analysis. *Sci. Rep.* **2019**, *9*, 10537. [[CrossRef](#)] [[PubMed](#)]
15. Adamski, N.M.; Borrill, P.; Brinton, J.; Harrington, S.A.; Marchal, C.; Bentley, A.R.; Bovill, W.D.; Cattivelli, L.; Cockram, J.; Contreras-Moreira, B.; et al. A roadmap for gene functional characterisation in crops with large genomes: Lessons from polyploid wheat. *eLife* **2020**, *9*, e55646. [[CrossRef](#)] [[PubMed](#)]
16. International Wheat Genome Sequencing Consortium (IWGSC); Appels, R.; Eversole, K.; Stein, N.; Feuillet, C.; Keller, B.; Rogers, J.; Pozniak, C.J.; Choulet, F.; Distelfeld, A.; et al. Shifting the limits in wheat research and breeding using a fully annotated reference genome. *Science* **2018**, *361*, eaar7191.
17. Li, C.; Li, L.; Reynolds, M.P.; Wang, J.; Chang, X.; Mao, X.; Jing, R. Recognizing the hidden half in wheat: Root system attributes associated with drought tolerance. *J. Exp. Bot.* **2021**, *72*, 5117–5133. [[CrossRef](#)] [[PubMed](#)]
18. Gabay, G.; Wang, H.; Zhang, J.; Moriconi, J.I.; Burguener, G.F.; Gualano, L.D.; Howell, T.; Lukaszewski, A.; Staskawicz, B.; Cho, M.J.; et al. Dosage differences in 12-OXOPHYTODIENOATE REDUCTASE genes modulate wheat root growth. *Nat. Commun.* **2023**, *14*, 539. [[CrossRef](#)] [[PubMed](#)]
19. Voss-Fels, K.P.; Robinson, H.; Mudge, S.R.; Richard, C.; Newman, S.; Wittkop, B.; Stahl, A.; Friedt, W.; Frisch, M.; Gabur, I.; et al. VERNALIZATION1 Modulates Root System Architecture in Wheat and Barley. *Mol. Plant* **2018**, *11*, 226–229. [[CrossRef](#)]
20. Wang, J.; Li, L.; Li, C.; Yang, X.; Xue, Y.; Zhu, Z.; Mao, X.; Jing, R. A transposon in the vacuolar sorting receptor gene *TaVSR1-B* promoter region is associated with wheat root depth at booting stage. *Plant Biotechnol. J.* **2021**, *19*, 1456–1467. [[CrossRef](#)]
21. Li, C.; Wang, J.; Li, L.; Li, J.; Zhuang, M.; Li, B.; Li, Q.; Huang, J.; Du, Y.; Wang, J.; et al. TaMOR is essential for root initiation and improvement of root system architecture in wheat. *Plant Biotechnol. J.* **2022**, *20*, 862–875. [[CrossRef](#)] [[PubMed](#)]
22. Fusi, R.; Rosignoli, S.; Lou, H.; Sangiorgi, G.; Bovina, R.; Pattem, J.K.; Borkar, A.N.; Lombardi, M.; Forestan, C.; Milner, S.G.; et al. Root angle is controlled by EGT1 in cereal crops employing an antigravitropic mechanism. *Proc. Natl. Acad. Sci. USA* **2022**, *119*, e2201350119. [[CrossRef](#)] [[PubMed](#)]
23. Kirschner, G.K.; Rosignoli, S.; Guo, L.; Vardanega, I.; Imani, J.; Altmüller, J.; Milner, S.G.; Balzano, R.; Nagel, K.A.; Pflugfelder, D.; et al. ENHANCED GRAVITROPISM 2 encodes a STERILE ALPHA MOTIF-containing protein that controls root growth angle in barley and wheat. *Proc. Natl. Acad. Sci. USA* **2021**, *118*, e2101526118. [[CrossRef](#)] [[PubMed](#)]
24. Zhuang, M.; Li, C.; Wang, J.; Mao, X.; Li, L.; Yin, J.; Du, Y.; Wang, X.; Jing, R. The wheat SHORT ROOT LENGTH 1 gene TaSRL1 controls root length in an auxin-dependent pathway. *J. Exp. Bot.* **2021**, *72*, 6977–6989. [[CrossRef](#)]
25. Ma, J.; Wang, Y.; Tang, X.; Zhao, D.; Zhang, D.; Li, C.; Li, W.; Li, T.; Jiang, L. TaSINA2B, interacting with *TaSINA1D*, positively regulates drought tolerance and root growth in wheat (*Triticum aestivum* L.). *Plant Cell Environ.* **2023**, *46*, 3760–3774. [[CrossRef](#)]
26. Xu, W.; Chen, Y.; Liu, B.; Li, Q.; Zhou, Y.; Li, X.; Guo, W.; Hu, Z.; Liu, Z.; Xin, M.; et al. *TaANR1-TaMADS25* module regulates lignin biosynthesis and root development in wheat (*Triticum aestivum* L.). *J. Genet. Genom.* **2023**, *50*, 917–920. [[CrossRef](#)]
27. Zhang, H.; Jin, Z.; Cui, F.; Zhao, L.; Zhang, X.; Chen, J.; Zhang, J.; Li, Y.; Li, Y.; Niu, Y.; et al. Epigenetic modifications regulate cultivar-specific root development and metabolic adaptation to nitrogen availability in wheat. *Nat. Commun.* **2023**, *14*, 8238. [[CrossRef](#)]
28. Zhao, P.; Ma, X.; Zhang, R.; Cheng, M.; Niu, Y.; Shi, X.; Ji, W.; Xu, S.; Wang, X. Integration of genome-wide association study, linkage analysis, and population transcriptome analysis to reveal the *TaFMO1-5B* modulating seminal root growth in bread wheat. *Plant J.* **2023**, *116*, 1385–1400. [[CrossRef](#)]
29. Wang, X.; Zhao, P.; Guo, X.; Liu, Z.; Ma, X.; Zhao, Y.; Lai, X.; Huang, L.; Wang, W.; Han, D.; et al. Population Transcriptome and Phenotype Reveal that the *Rht-D1b* Contribute a Larger Seedling Roots to Modern Wheat Cultivars. *bioRxiv* **2022**, 2022.06.02.494553.
30. Zhao, P.; Liu, Z.; Shi, X.; Hou, W.; Cheng, M.; Liu, Y.; Simmonds, J.; Ji, W.; Uauy, C.; Xu, S.; et al. Modern wheat breeding selection synergistically improves above- and below-ground traits. *bioRxiv* **2023**, 2023.2010.2027.564104.
31. Zhu, T.; Wang, L.; Rimbart, H.; Rodriguez, J.C.; Deal, K.R.; De Oliveira, R.; Choulet, F.; Keeble-Gagnère, G.; Tibbits, J.; Rogers, J.; et al. Optical maps refine the bread wheat *Triticum aestivum* cv. Chinese Spring genome assembly. *Plant J.* **2021**, *107*, 303–314. [[CrossRef](#)] [[PubMed](#)]
32. Ramirez-Gonzalez, R.H.; Uauy, C.; Caccamo, M. PolyMarker: A fast polyploid primer design pipeline. *Bioinformatics* **2015**, *31*, 2038–2039. [[CrossRef](#)] [[PubMed](#)]
33. Chen, Y.; Song, W.; Xie, X.; Wang, Z.; Guan, P.; Peng, H.; Jiao, Y.; Ni, Z.; Sun, Q.; Guo, W. A Collinearity-Incorporating Homology Inference Strategy for Connecting Emerging Assemblies in the Triticeae Tribe as a Pilot Practice in the Plant Pangenomic Era. *Mol. Plant* **2020**, *13*, 1694–1708. [[CrossRef](#)] [[PubMed](#)]

34. Zipfel, C.; Kunze, G.; Chinchilla, D.; Caniard, A.; Jones, J.D.; Boller, T.; Felix, G. Perception of the bacterial PAMP EF-Tu by the receptor EFR restricts *Agrobacterium*-mediated transformation. *Cell* **2006**, *125*, 749–760. [[CrossRef](#)]
35. Ma, J.F.; Yamaji, N.; Mitani, N.; Tamai, K.; Konishi, S.; Fujiwara, T.; Katsuhara, M.; Yano, M. An efflux transporter of silicon in rice. *Nature* **2007**, *448*, 209–212. [[CrossRef](#)] [[PubMed](#)]
36. Yamaji, N.; Sakurai, G.; Mitani-Ueno, N.; Ma, J.F. Orchestration of three transporters and distinct vascular structures in node for intervascular transfer of silicon in rice. *Proc. Natl. Acad. Sci. USA* **2015**, *112*, 11401–11406. [[CrossRef](#)] [[PubMed](#)]
37. Morris, E.R.; Chevalier, D.; Walker, J.C. DAWDLE, a forkhead-associated domain gene, regulates multiple aspects of plant development. *Plant Physiol.* **2006**, *141*, 932–941. [[CrossRef](#)]
38. Zäuner, S.; Ternes, P.; Warnecke, D. Biosynthesis of sphingolipids in plants (and some of their functions). *Adv. Exp. Med. Biol.* **2010**, *688*, 249–263.
39. Saluja, M.; Zhu, F.; Yu, H.; Walia, H.; Sattler, S.E. Loss of COMT activity reduces lateral root formation and alters the response to water limitation in sorghum brown midrib (bmr) 12 mutant. *New Phytol.* **2021**, *229*, 2780–2794. [[CrossRef](#)]
40. van Hengel, A.J.; Roberts, K. AtAGP30, an arabinogalactan-protein in the cell walls of the primary root, plays a role in root regeneration and seed germination. *Plant J.* **2003**, *36*, 256–270. [[CrossRef](#)]
41. Li, Y.; Zhou, J.; Li, Z.; Qiao, J.; Quan, R.; Wang, J.; Huang, R.; Qin, H. SALT AND ABA RESPONSE ERF1 improves seed germination and salt tolerance by repressing ABA signaling in rice. *Plant Physiol.* **2022**, *189*, 1110–1127. [[CrossRef](#)] [[PubMed](#)]
42. Xu, K.; Chen, S.; Li, T.; Ma, X.; Liang, X.; Ding, X.; Liu, H.; Luo, L. OsGRAS23, a rice GRAS transcription factor gene, is involved in drought stress response through regulating expression of stress-responsive genes. *BMC Plant Biol.* **2015**, *15*, 141. [[CrossRef](#)] [[PubMed](#)]
43. Motte, H.; Vanneste, S.; Beeckman, T. Molecular and Environmental Regulation of Root Development. *Annu. Rev. Plant Biol.* **2019**, *70*, 465–488. [[CrossRef](#)] [[PubMed](#)]
44. Liu, Z.; Zhao, P.; Lai, X.; Wang, X.; Ji, W.; Xu, S. The selection and application of peduncle length QTL *QPL_6D.1* in modern wheat (*Triticum aestivum* L.) breeding. *Theor. Appl. Genet.* **2023**, *136*, 32. [[CrossRef](#)] [[PubMed](#)]
45. Ma, J.; Zhao, D.; Tang, X.; Yuan, M.; Zhang, D.; Xu, M.; Duan, Y.; Ren, H.; Zeng, Q.; Wu, J.; et al. Genome-Wide Association Study on Root System Architecture and Identification of Candidate Genes in Wheat (*Triticum aestivum* L.). *Int. J. Mol. Sci.* **2022**, *23*, 1843. [[CrossRef](#)] [[PubMed](#)]
46. Xu, F.; Chen, S.; Yang, X.; Zhou, S.; Wang, J.; Zhang, Z.; Huang, Y.; Song, M.; Zhang, J.; Zhan, K.; et al. Genome-Wide Association Study on Root Traits Under Different Growing Environments in Wheat (*Triticum aestivum* L.). *Front. Genet.* **2021**, *12*, 646712. [[CrossRef](#)] [[PubMed](#)]
47. Cui, K.; Huang, J.; Xing, Y.; Yu, S.; Xu, C.; Peng, S. Mapping QTLs for seedling characteristics under different water supply conditions in rice (*Oryza sativa*). *Physiol. Plant* **2008**, *132*, 53–68. [[CrossRef](#)] [[PubMed](#)]
48. Beyer, S.; Daba, S.; Tyagi, P.; Bockelman, H.; Brown-Guedira, G.; Mohammadi, M. Loci and candidate genes controlling root traits in wheat seedlings—a wheat root GWAS. *Funct. Integr. Genom.* **2019**, *19*, 91–107. [[CrossRef](#)]

Disclaimer/Publisher’s Note: The statements, opinions and data contained in all publications are solely those of the individual author(s) and contributor(s) and not of MDPI and/or the editor(s). MDPI and/or the editor(s) disclaim responsibility for any injury to people or property resulting from any ideas, methods, instructions or products referred to in the content.